A New Method of Current Density Distribution for Switched Reluctance Machine to Increase Average output Torque

Guangjin Li, Javier Ojeda, Emmanuel Hoang, Michel Lécrivain, Mohamed Gabsi

A New Method of Current Density Distribution for Switched Reluctance Machine to Increase Average output Torque

GuangJin LI, Xavier OJEDA, Emmanuel HOANG, Michel LECRIVAIN, Mohamed GABSI
SATIE, ENS Cachan, 61, av President Wilson, F-94230 Cachan, France

Abstract – The electromagnetic performances for two current distribution methods (classical and non-classical) of a 3-phase, 24 stator slots and 16 rotor poles Switching Reluctance Machine (SRM) were compared. The three phases were excited in sinusoidal current mode. The Finite Element Model was used to predict the average torque, the total flux of each phase, the torque ripple, the self and the mutual-inductance of each phase. After the computation, it is shown that the machine with non-classical current distribution has more average torque than the machine with classical current distribution, especially at high current density. Experimental tests have been realized, and a good agreement between the experimental and numerical (FE) results was observed.
Keywords: Switching Reluctance Machine, Finite Element Model, average torque, torque ripple, self and mutual-inductance, flux in air-gap.

I. Introduction

Nowadays, the Switching Reluctance Machines (SRMs) become an important topic for the researchers of electrical machines because of their advantages: simplicity, robustness, high speed operation and low manufacturing cost, etc. However, the disadvantages of this kind of machines are high torque ripple, high acoustical noise and vibration which limit their applications in industry [1], [2].

The SRMs to be investigated have the same geometrical structure but are excited in two different ways of current distribution as Figure 1 and table 1 [3], the machine parameters are expressed in table 2.

Table 1: current distribution of SRM

Classical	A'ABB'C'CAA'B'BCC'
Non-classical	AA'BB'CC'AA'BB'CC'

Table 2: machine parameters

	24-slot/16-pole
Slot number	24
Pole number	16
Air gap length	0.2 mm
Stack length	60 mm
Stator outer radius	45 mm
Stator inner radius	29.2 mm
Rotor outer radius	29 mm

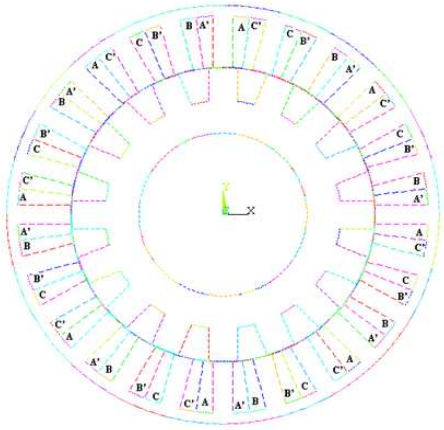

(a)

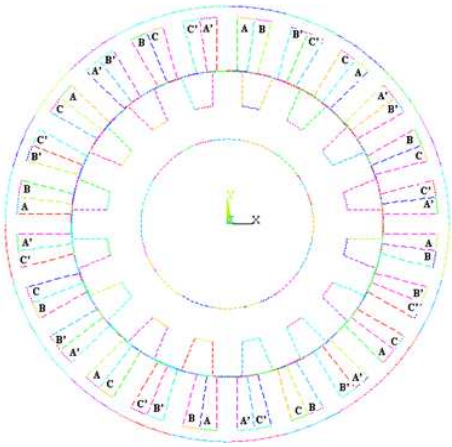

(b)

Figure 1: the current distribution for SRMs (a) non classical (b) classical

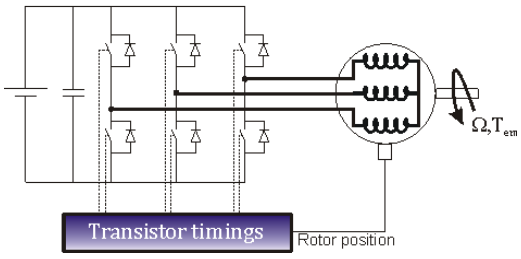

Figure 2: excitation for the SRM in sinusoidal current mode

In this paper, the excitation of three-phase is achieved in a sinusoidal current mode as shown

in Figure 2 in order to simplify the inverter circuit and minimize the saturation of SRMs [4].

The analysis of nonlinear characteristics is based on Finite Element Model (FEM), and the results from ANSYS are employed to practice the design and optimization of SRM system.

II. Flux-Linkage

The coil is wound around a stator tooth, thus, when the stator and the rotor teeth are aligned, the flux-linkage is maximum. This value depends on the tooth tip's width and the air gap field. The equation of the flux per coil is expressed as:

$$\varphi_{1coil} = \int_S \vec{B}_{airgap} d\vec{S}_{teeth} \qquad \text{Eq. 1}$$

Where B_{airgap} is the air gap flux-density and S_{teeth} is the teeth tips surface area.

In 2-D analysis, $\psi(\theta, i)$ can be calculated with the magnetic vector potential A, and the final expression of flux-linkage is obtained by:

$$\psi_{1phase} = N \cdot \int_S \vec{B}_{airgap} d\vec{S}_{teeth} = N \cdot \int_l \vec{A} \cdot d\vec{L} \qquad \text{Eq.2}$$

Typical flux distributions at aligned position and the flux of one phase versus RMS current density for the 24-slot and 16-pole three-phase SRM with different ways of excitation are shown in Figure 3 and in Figure 4, respectively.

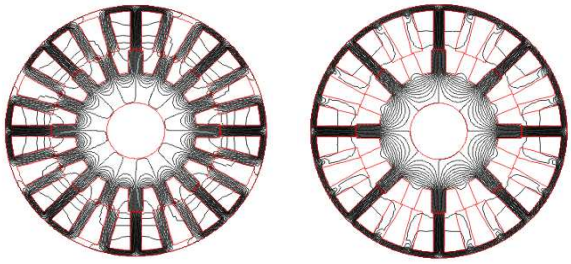

(a) (b)

Figure 3: Flux distributions in aligned position of SRM. (a) Non-classical current density distribution (b) Classical current density distribution.

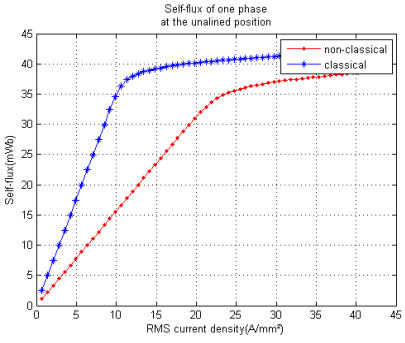

(a) Self-flux of one phase

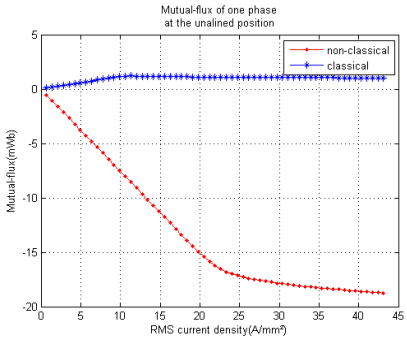

(a) Mutual-flux of one phase

Figure 4: Self and mutual-flux of one phase with single excited phase (in this paper, phase A is excited)

In the Figure 3, for the non-classical current distribution machine, it is clear that each half of phase A flux goes through the phase B or the phase C, as a result, the mutual flux is about the half of the self flux. This is different from the classical current distribution machine. In the last case, approximately all the flux passes through the different teeth of the phase A, thus, the mutual flux is very low, can be neglected. The previous assumption is well justified by the Figure 4. At the same time, we find that the self and mutual flux of the non-classical current distribution is much less sensitive to the increase of current density. Due to this characteristic, we can finally obtain more out-put torque at high current density. This will be discussed in part-IV.

III. Self and Mutual Inductances

The self and mutual-inductance are calculated with the same expressions although the current distribution of the two SRMs is different.

$$\psi_{1phase} = L_1 \cdot I = N^2 \cdot p_1 \cdot I = N \cdot \varphi_{1coil} \qquad \text{Eq. 3}$$

And the fluxes between two phases are calculated as:

$$\psi_{1\_i\_phase} = M_{1\_i} \cdot i_1 = N^2 \cdot p_{1\_i} \cdot i_1 = N \cdot \varphi_{1\_i\_coil} \qquad \text{Eq.4}$$

(i=2, 3)

Finally, the self-permeance and mutual-permeance are calculated as:

$$p_1 = \varphi_{1coil} / N \cdot i_1 \quad \text{and} \quad p_{1\_i} = \varphi_{1\_i\_coil} / N \cdot i_1$$

After the simulation in ANSYS, the wave-form of the permeance is shown in Figure 5. On one hand, the variation of self-permeance of classical distribution ($\Delta p = 3 \times 10^{-5}$ Wb/A) is more significant than non-classical distribution ($\Delta p = 1 \times 10^{-5}$ Wb/A), and the value is about 3 times. On the other hand, the variation of the mutual-permeance of classical distribution ($\Delta p_{12} = \Delta p_{13} = \Delta p_{23} = 0.48 \times 10^{-}$

^{6}Wb/A) is less significant than non-classical distribution (Δp_{ii}=1.33x10^{-6}Wb/A, i=1,2,3), the value is about 0.36 times.

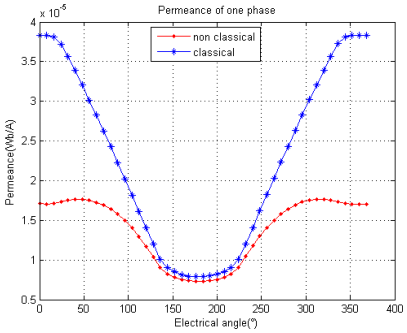

(a)

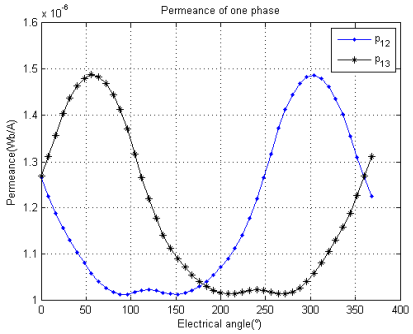

(b)

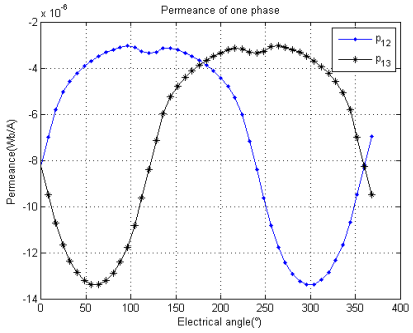

(c)

Figure 5: the self-permeance and mutual-permeance for the effective current density JS=7.07A/mm² (a) self-permeance of classical and non-classical distribution current (b) mutual-permeance of classical distribution (c) mutual-permeance of non-classical distribution.

IV. Output torque and torque ripple

The magnetic energy is stocked in the air gap of SRM, and the torque can be computed from the co-energy derivative with θ (angular position of rotor) as [5]:

$$T(\theta,i)=\frac{\partial W'(\theta,i)}{\partial \theta}\Big|_{i=const} \qquad \text{Eq. 5}$$

Where W'(θ,i) is a function of the angular positions of the rotor and the current i, and that is computed without saturation as:

$$W'(\theta,i)=\tfrac{1}{2}N^2p_1(\theta)\cdot i_1^2+\tfrac{1}{2}N^2p_2(\theta)\cdot i_2^2+\tfrac{1}{2}N^2p_3(\theta)\cdot i_3^2+ N^2/p_{12}(\theta)\cdot i_1\cdot i_2+N^2/p_{13}(\theta)\cdot i_1\cdot i_3+N^2/p_{23}(\theta)\cdot i_2\cdot i_3 \qquad \text{Eq.6}$$

Finally, the expression of torque is obtained as:

$$T(\theta,i)=\tfrac{1}{2}\frac{\partial N^2p_1(\theta)}{\partial\theta}\cdot i_1^2+\tfrac{1}{2}\frac{\partial N^2p_2(\theta)}{\partial\theta}\cdot i_2^2+\tfrac{1}{2}\frac{\partial N^2p_3(\theta)}{\partial\theta}\cdot i_3^2 +\frac{\partial N^2/p_{12}(\theta)}{\partial\theta}\cdot i_1\cdot i_2+\frac{\partial N^2/p_{13}(\theta)}{\partial\theta}\cdot i_1\cdot i_3+\frac{\partial N^2/p_{23}(\theta)}{\partial\theta}\cdot i_2\cdot i_3 \qquad \text{Eq.7}$$

Where $L_i/N^2 = p_i$, $N^2/M_{ii} = p_{ii}$, (i=1, 2, 3), p_i and p_{ii} are respectively the self-permeance and mutual-permeance. From the Eq.7, the torque is determined by the variations of the self and mutual-permeance. As we have discussed in part-III, the non-classical distribution SRM utilises the mutual-inductance rather than self-inductance to produce the output torque [6]. This is opposite to the classical current distribution of SRM. The numerical results from ANSYS like the wave-form of the average torque and the wave-form of the instantaneous output torque are shown in the Figure 6 and in the Figure 7, respectively.

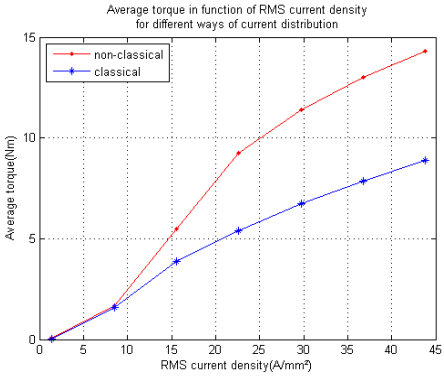

Figure 6: Average torque versus RMS current density of the two different types of current distribution at the stack length equals to 60mm

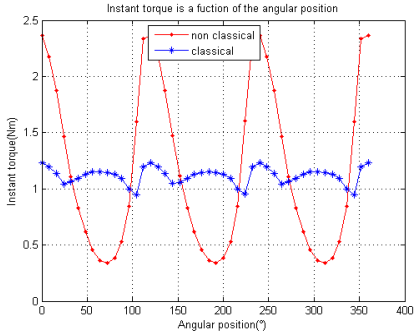

(a) Instantaneous torque at low current density

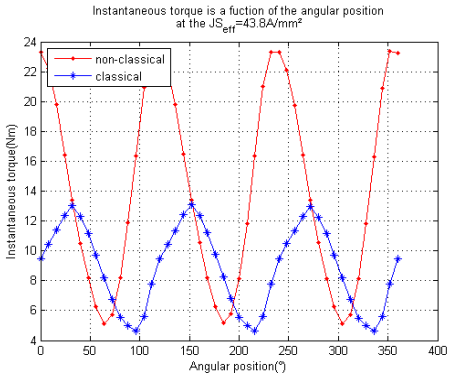

(b) Instantaneous torque at high current density

Figure 7: Instantaneous out-put torque of the two different types of current distribution at (a) the RMS current density JS=7.07A/mm² and at (b) the RMS current density JS=43.8A/mm²

The ratio of torque ripple is computed as:

$$\Delta T = \frac{T\max - T\min}{T_{av}} \qquad \text{Eq. 8}$$

Where T_{max} is the maximum torque, T_{min} is the minimum torque and T_{av} is the average torque.

In Figure 8, the non-classical current distribution of SRM has more torque ripple than the classical current distribution at low average out-put torque (low current density). With the increase of current density, the torque ripple of two machines is not important.

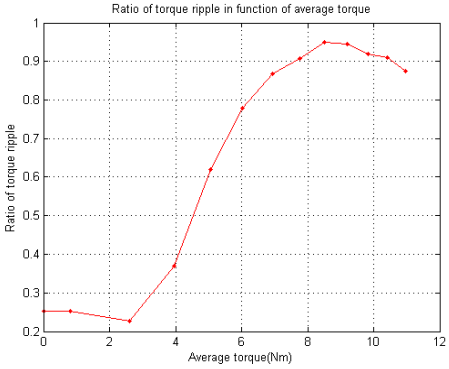

(a) Classical current distribution

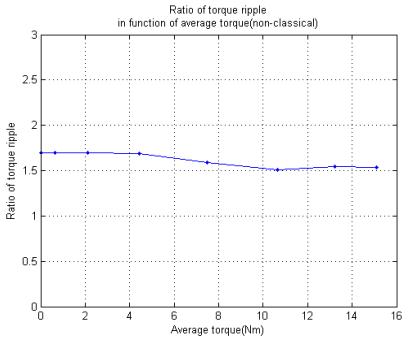

(b) Non-classical current distribution

Figure 8: Ratio of torque ripple versus average out-put torque

As seen, when the current density is low, for example, JS=7A/mm², the self and mutual-inductance are unsaturated, the difference of output average torque is not significant, the average torque of non-classical distribution (T=1.15Nm) is only 5% greater than the classical distribution (1.09Nm). At the same time, the ratio of torque ripple of the non-classical distribution is 1.7 which is 6.8 times greater than that of the classical distribution, the last whose torque ripple is only 0.25. When the RMS current density increases, as we have discussed in part-II, the non-classical current distribution machine begins to saturate, the variations of the self and mutual-inductance become poor, which leads to a lower out-put average torque. Because of the non-sensitive characteristic to the increase of current density, the non-classical current distribution machine stays unsaturated. As a result, the variations of self and mutual-inductance are great, which finally leads to a higher out-put average torque. The more the current density is high, the more the out-put average torque of the non-classical current distribution is greater than that of the classical current distribution machine, until the non-classical current distribution machine is also saturated, for example, JS=43.8A/mm². At JS=43.8A/mm², the out-put average torque of non-classical current distribution machine (T=14.3Nm) is 61% greater than that of classical current distribution machine (T=8.9Nm), and the ratio of torque ripple of the non-classical distribution (1.55) is only 1.7 times greater than that of classical distribution (0.88). The high out-put average torque and a relatively lower ratio of torque ripple is very useful for the starter-generator application.

V. Experimental validation on a small 3-phase Switching Reluctance Machine

In order to validate our previous assumptions and numerical results, we have realized experimental test. In our laboratory, the available machine is a 3-phase, 6-stator poles and 4-rotor poles Switching Reluctance Machine, which is shown in Figure 9. It has a stator outer diameter of 120mm, a rotor outer diameter of 66mm, an axial active length of 60mm, and the nominal out-put torque of 0.1Nm. In order to compare the experimental SRM with the proposed SRM in this paper, the curves are normalised (p.u.) and plotted in one electrical period. Thus, the two SRMs waveforms are similar, but the amplitude and the mechanical period of the real values are different. The comparisons are shown in Figure 10 and Figure 11.

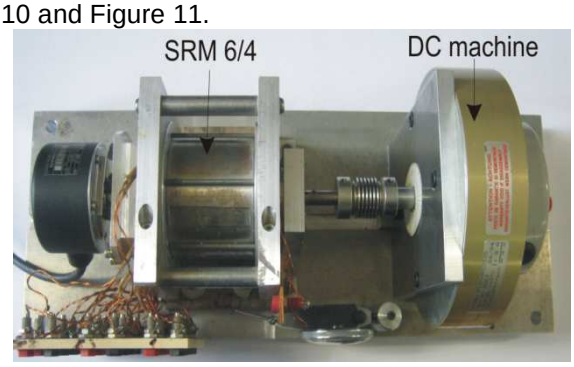

Figure 9: Small 3-phase experimental SRM

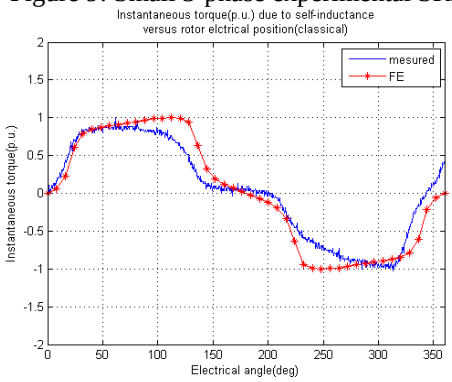

(a) Torque due to self-inductance

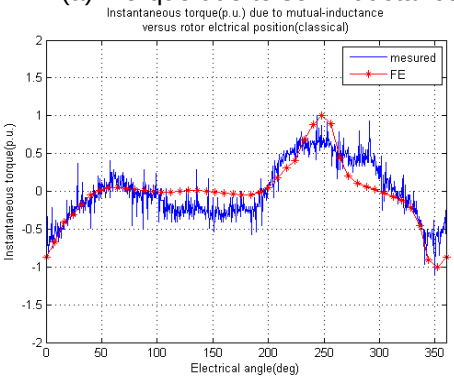

(b) Torque due to mutual-inductance

Figure 10: Instantaneous torque (p.u.) versus rotor electrical position of the classical current distribution SRM at constant current

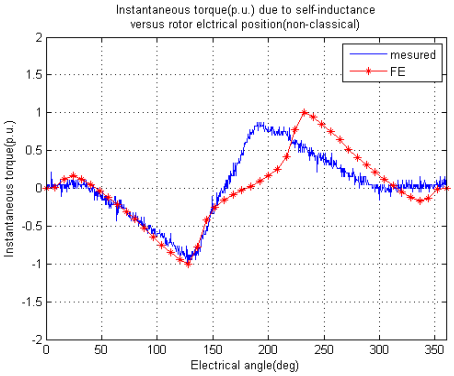

(a) Torque due to self-inductance

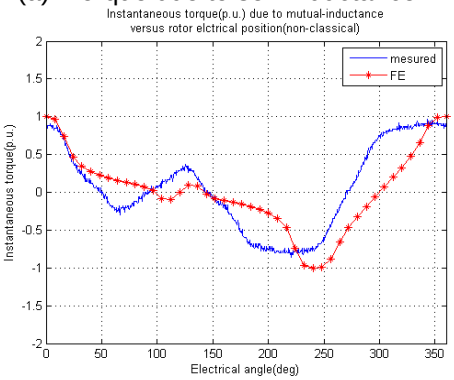

(b) Torque due to mutual-inductance

Figure 11: Instantaneous torque (p.u.) versus rotor electrical position of the classical current distribution SRM at constant current

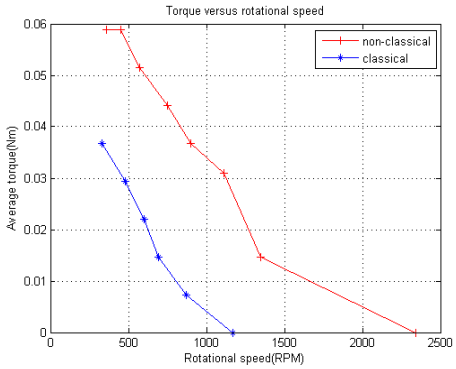

Figure 12: Average out-put torque versus rotational speed

After the comparison of the experimental and numerical (FE) results, a good agreement was observed, thus, the previous conclusions obtained from FE results is valid. From the Figure 12, we find that the non-classical current distribution SRM has a speed range two times larger than that of the classical current distribution SRM. This is a very attractive

advantage for the high speed operation (aerospace application).

VI. Conclusion

The performance of different kinds of current distribution for the three-phase SRMs with 24-slot and 16-pole has been presented in this paper. It has shown that the different kinds of current distribution have an important influence over the performance of SRMs. When SRMs are saturated, the output torque of the non-classical distribution SRM is much greater than that of the classical distribution SRM. This is very useful for the starter-generator application (aerospace or Hybrid vehicle). At the same time, the torque ripple of the non-classical distribution is also relatively higher. After our experimental tests, a good agreement between the experimental and the numerical (FE) results was observed, and the non-classical current distribution SRM has a speed range two times larger than that of classical current distribution. Moreover, a prototype of the 3-phase SRM with 24 stator poles and 16 rotor poles will be constructed, and the optimization will also be done.

REFERENCES

[1] X. OJEDA, X. MININGER, M. GABSI, M. LECRIVAIN, ''*Sinusoidal Feeding for Switched Reluctance Machine: Application to Vibration Damping*'' ICEM 2008, Vilamoura, Portugal, September 2008.

[2] Z. Q. Zhu and D. Howe, ''*Electrical Machines and Drives for Electric, Hybrid, and Fuel Cell Vehicles,*'' Proc. IEEE, vol. 95, no. 4, pp. 746-765, Apr. 2007.

[3] J. Cros and P. Viarouge, ''*Synthesis of High Performance PM motors With Concentrated Windings,*'' IEEE Trans. Energy Convers., vol. 17, no. 2, pp. 248-253, jun. 2002.

[4] M. GABSI, A. D. VRIES, M. L. PINCART, Y. BONNASSIEUX, M. LECRIVAIN, C. PLASSE "*Sine Wave Current Feeding of Doubly Salient Switched Reluctance Machines. Application to the Car Starter Generator,*" CD proceeding of ICEM'04, 5-8 september, CRACOW, Polond.

[5] J. J. Zhang, H. J. Zhang, R. Z. Gao and L. L. Wang, ''*Control Simulation Studies for Switched Reluctance Motor System Based on Finite Element Model,*'' Proceeding of International Conference on Power Electronics, Machines and Drives PEMD 2008, York, UK. 2-4, Apr. 2008, 169-173.

[6] B. C. Mecrow, ''*New Winding Configurations for Doubly Salient Reluctance Machines,*'' IEEE Trans. Ind. Appl., vol. 32, no. 6, pp. 1348–1356, Nov./Dec. 1996.

About the authors

Guangjin LI was born in Xiaogan, China, in 1984. He received his MSc degree in Electrical Engineering from the University of Paris XI, Paris, France, in 2008. He is currently a PHD student in the laboratory SATIE of the Ecole Normale Supérieure (ENS) de Cachan, Paris, France. His main research interests include the design and the optimization of the Switching Reluctance Machines (SRMs) and the Flux-Switching Permanent Magnet Machines (FSPMMs). The available contact of the author is: guangjin.li@satie.ens-cachan.fr

Xavier Ojeda was born in 1980 in Buenos Aires, Argentina. He received the BS and the MSc degrees in electrical engineering from the Ecole Normale Supérieure de Cachan (ENS Cachan, France) and Paris-XI University. He is actually preparing his Phd in Electrical Engineering in SATIE, Systèmes et Applications des Technologies de l'Information et de l'Energie (ENS Cachan, France), laboratory. His main research topics are active damping of SRM motors for high speed applications and machines noise modelling.

Emmanuel Hoang was born in Antibes, France, in 1966. He receive the ''agrégation'' in electrical engineering in 1990 and the Ph.D degrees fromm the Ecole Normale Supérieure de Cachan, in 1995. Since 1990, he works with the electrical machine team in the SATIE laboratory. His research interests the modelling of the iron losses in SRMs and the design, modelling, optimisation and control of novel topologies of PM machines. hoang@satie.ens-cachan.fr

Mohamed Gabsi received his PhD degree in electrical engineering from University of Paris-VI in 1987 and his HDR in 1999 from University of Paris-XI (Orsay, France). Since 1990, he is working in electrical machine team (SETE, Systèmes d'´Energies pour le Transport et l'Environnement) of SATIE laboratory where he is currently a professor and researcher. His research interests include SRM, vibrations and acoustic noise and PM machines.

Michel Lécrivain was born in Barneville, France. He received the degree in electrical engineering from the Conservatoire National des Arts et Métiers (CNAM, Paris, France) in 1981. He has joined since 1997, SATIE laboratory as a research engineer. His research interests include the design and control of new hybrid machines and novel permanent magnet machines for automotive applications.